Available online at www.sciencedirect.com
SCIENCE DIRECT®
Polymer 45 (2004) 2413–2425
polymer
www.elsevier.com/locate/polymer

Effects of crystallization behavior on morphological change in poly(trimethylene terephthalate) spherulites

Wei-Tsung Chuang[a], Po-Da Hong[a,*], Hoe H. Chuah[b]

[a]*Department of Polymer Engineering, National Taiwan University of Science and Technology, Taipei 10607, Taiwan*
[b]*Shell Chemical Company, Houston, TX 77251, USA*

Received 5 August 2003; received in revised form 28 November 2003; accepted 5 January 2004

Abstract

In poly(trimethylene terephthalate) (PTT) spherulites during isothermal crystallization, the morphological changed from an axialite/or elliptical banded spherulite to banded spherulite and then non-banded spherulite with temperature decreasing were studied by following the lamellar growth behaviors. We report lamellar growth mechanism on varied crystallization temperature, which explicitly probes the link between microscopic structure and macroscopic morphology in the development of patterns. Fibrillation of the edge-on lamellae was observed on the surfaces of axialite and the convex bands of banded spherulite. Terrace-like lamellae were observed on the surface of the non-banded spherulite and the concave bands of banded-spherulite. In thin film crystallization, PTT banded spherulite exhibits a texture of alternate edge-on and flat-on lamellae, wavy-like surface and rhythmic growth. The deceleration of growth rate takes place in convex bands with a growth habit of fibrillation of the edge-on lamellae for emerging ridge surface. On the other hand, the acceleration of growth rate appears in concave bands with a growth habit of terrace-like lamellae for emerging valley surface. The alternating growth mechanism of the lamellae was considered to be related with the formation of spatiotemporal self-organization patterns far from equilibrium. In order to explain the rhythmic growth and periodic growth of the lamellae, we may conjecture that the emergence of PTT banded spherulite in thin film crystallization is associated with an oscillatory dynamics of the spherulite growth front driven by latent heat diffusion. We present some tentative ideas on the possibility of band-to-nonband (BNB) morphological transition, which might be analogous with the second order transition in non-equilibrium phase transition.
© 2004 Elsevier Ltd. All rights reserved.

Keywords: Poly(trimethylene terephthalate); Spherulites; Polymers

1. Introduction

Banded spherulite exhibits a macroscopic morphology with concentric rings or bands. It can be found in many kinds of materials such as polymers [1–5], inorganic matters [6,7] and liquid crystals [8]. The periodic change in the birefringence along the radius of a polyethylene spherulite was explained by Keller [1,9] as due to the regular, smooth twisting of lamellae along the radial direction. From microscopy studies, Bassett et al. [4,10,11] showed that the polyethylene banded spherulites consisted of the untwisted *S*- or *C*-profiled lamellae. The origin of the twisted or the untwisted banded spherulite had been postulated as being caused by surface stresses [12,13], spiral terraces [14,15], giant screw dislocations [16,17], isochiral dislocations [18,19] and so on. Recently, Keith [20] commented on the simulation by revisiting two topics: (a) the origins of secondary effects of rhythmic character in thin films and (b) the generation of isochiral dislocation and torsion in twisted lamellae, to clarify the various interpretations of the origins of banded spherulite.

In nature, there are many systems found common phenomenon of banded or ringed patterns, such as spiral waves in the Belousov–Zhabotinsky (B–Z) redox reaction [21–23], Rayleigh–Benard convection cells in heated fluids [21–23], Liesegang rings in reaction-diffusion systems [24], and banded structure in solidification alloys [25–29]. Kyu et al. [30] have suggested already that banded spherulites not only exhibit concentric bands but also exhibit rhythmic growth, which is characterized by a fast growth followed by a slow growth. They considered that the similarities

* Corresponding author. Tel.: +886-2-27376539; fax: +886-2-27376544.
E-mail address: poda@mail.ntust.edu.tw (P.D. Hong).

0032-3861/$ - see front matter © 2004 Elsevier Ltd. All rights reserved.
doi:10.1016/j.polymer.2004.01.048

between the rhythmic growth in banded spherulites and target /or spiral growth patterns in B–Z redox reactions suggest a useful viewpoint of crystallization under non-equilibrium conditions. Underlying many disparate patterns, Ben-Jacob [31] suggested a set of overarching principles that can lend a unified perspective. This may drive us to consider whether other phenomena could draw an analogy with the growth process of banded spherulites.

From the previous studies on PTT crystallization [32], we found that the morphology of crystallite was changed sharply from either an axialite crystallite or an elliptically shaped spherulite to a banded and then a non-banded spherulite as isothermal crystallization temperature T_{iso} was decreased. Although band-to-nonband (BNB) morphology transition has been seen in many systems [7,33–36], there are fewer detail studies on how the crystallization temperature influences macroscopic organization of crystallites. One possibility is that there is a smooth crossover, where all quantities vary analytically with the degree of undercooling ΔT. In polymeric crystallization, theories of kinetics-limited growth, where the rate of freezing is limited by local attachment kinetics [37], typically predicts such crossovers. Another possibility is that morphologies may vary non-analytically with ΔT.. It has analogy with equilibrium phase transitions [38–41]. Different morphologies are then the result of distinct growth mechanisms. It is well known that systems driven far from equilibrium can undergo dissipative transitions analogous to the first and second order phase transitions [42–45]. Hutter and Bechhoefer [46,47] also reported that the transition between banded and non-banded spherulitic growth in liquid crystals is analogous to a second-order transition. It is worthily investigating the banded formation of polymeric crystallization from a new perspective.

In this study, we are interested to note how the microscopic organization affects macroscopic pattern with changing crystallization temperature, since the macroscopic morphology is formed through microscopic lamellar structure. Furthermore, we would discuss the BNB morphological transition of PTT spherulites from a new perspective of non-equilibrium morphology transition. Our focus might ask whether, by BNB transition analogy to equilibrium transitions, a full range of non-equilibrium exponent could be obtained, and whether their behaviors obey the scaling relation.

2. Experimental section

2.1. Materials

Polytrimethylene terephthalate (PTT), supplied by Shell Chemical Company, has an intrinsic viscosity of 0.92 dl/g (measured in 60/40 phenol/tetrachloroethane at 333 K). The polymer was melt polymerized by the polycondensation of 1,3-propanediol with purified terephthalic acid. Other than the presence of the polymerization catalysts at ppm level, the polymer was free of additives, such as TiO_2, which could affect the polymer's crystallization behavior. The samples were first dried at 363 K for 6 h under vacuum before carrying out any new thermal treatments or experimental characterizations to minimize hydrolytic degradation of the melt.

2.2. Measurements

PTT spherulite's growth and morphologies were studied using a Leica Laborlux 12 Pols Polarized Light Microscope (PLM), equipped with a Linkam THMS 600 hot-stage. PTT thin film, ~10 μm thick, was melted at 553 K in the hot stage for 5 min and then rapidly cooled to the desired crystallization temperature. Spherulite growth images were recorded under transmission light with a CCD camera as a function of time until the spherulites impinge on each other. When taking the reflected light (RLM) optical images, the microscope's light source was simply changed to the reflective mode.

Nano-scale morphology of the spherulites was studied using the Atomic Force Microscopy (AFM). Since the AFM resolution, especially at the nm level, is improved by having a smooth sample surface, PTT thin film with the smoothest surface possible was prepared using the following steps: A thin slice of PTT was shaved from the polymer chip; it was then sandwiched and melted between two glass slides in the Linkam hot stage which was continuously purged with dry nitrogen to minimize thermo-oxidative degradation of the melt. After cooling, one of the glass slides was removed. The thin film sample, ~10 μm thick, was then heated to 553 K for 5 min. The temperature was then rapidly quenched to the desired crystallization temperature.

Tapping mode AFM was used to obtain both the height and phase images simultaneously using a Digital Instruments NanoScope III with a Multimode scanning probe setup. Silicon probes (Nanoprobes, Digital Instruments) with 125 μm-long cantilevers and resonance frequencies from 270 to 350 kHz were used. To image the nano-scale morphology, probes with very small tip radii of 5–10 nm were used. The set-point amplitude, A_{sp} was set at 0.4–0.6 of the free oscillation amplitude, A_0. The data were collected at 512×512 pixels per image, and the scan frequency was 0.2 ~ 1 Hz. In the tapping mode, the tip made intermittent contacts with the surface to obtain the height images to reveal the surface corrugations and morphology. Phase lag of the cantilever oscillation, relative to the signal sent to the cantilever's piezoelectric driver, was simultaneously monitored to obtain the phase images. Since phase lag was very sensitive to the variations of material properties such as stiffness and density, phase imaging was useful in differentiating the various component phases [48]. The technique was, therefore, used to image the lamellae and its amorphous surrounding.

3. Results

3.1. Crystallization kinetics and morphological change of crystallites

In the previous study [49], we reported that PTT exhibits three crystallization regimes depending on the melt crystallization temperature, T_{iso}. The regimes I → II and II → III transitions occurred at 488 and 468 K, respectively. We also reported PTT's average growth rate, G, and its Avrami rate constant, k, for both cold- and melt-crystallizations. By combining those results with the present AFM and optical microscopy studies of the crystallites formed in these three regimes, a PTT crystallization kinetic phase diagram is constructed as shown in Fig. 1. When a quenched, fully amorphous PTT was heated above its glass transition to induce cold-crystallization, AFM phase imaging showed that it formed a sheaf-like structure. Meanwhile, PTT was crystallized from the melt; the three crystallization regimes exhibited various spherulitic morphologies. As T_{iso} was decreased, the morphology changed from either an axialite structure or an elliptically shaped spherulite in regime I to a banded and a non-banded spherulite in regimes II and III, respectively. The transition of a banded to a non-banded spherulite took place at $T_{iso} = 468$ K. It is interesting to note that each crystallization regime has its own characteristic morphology. The variation in the temperature dependence of crystallization rate leading to the change in crystallite morphology was common phenomenon in many systems [47,50,51]. In fact, there is no conclusive proof to consider that the cause of banded spherulites is related to regime behavior. Therefore, this experimental result may be a coincidence only. In the present study, our discussion is based on the free surface. To learn about it, we carried out AFM studies to see microscopic mechanism of lamellar growth change at a higher resolution. Bearing in mind, this technique probed only the surface morphology of the spherulite; the interpretation of the bulk morphology has to be supplemented with other techniques. All AFM's results in lamellar structures were double-checked in order to avoid surface pseudomorph. The surface structures of lamellae and macroscopic morphology, investigated by AFM and optical microscopy, respectively, are presented below.

3.2. Non-banded spherulites

PTT non-banded spherulite was formed only at $T_{iso} < 468$ K. Fig. 2 showed the AFM phase image of the non-banded spherulite crystallized at $T_{iso} = 453$ K. In AFM images, the lighter regions could be interpreted as regions that were either high in topography or high in phase lag response from the stiffer lamellar crystals. In Fig. 2(a), 5×5 μm^2 scan size, PTT's non-banded spherulite's surface was rather smooth compared to the corrugated-like surface of banded spherulite and did not exhibit a fibrillar morphology like those in the banded spherulite (see later). However, at Fig. 2(a)'s magnification details of the lamellar organization could not be clearly observed. The phase image of Fig. 2(b), 500×500 nm^2 scan size, showed that the non-banded spherulite's surface often, although there is a sporadic protuberance of surface, has flat-on lamellae. The growth direction of flat-on lamellae was parallel to the substrate plane. The three dimension height images of AFM corresponding to Fig. 2(b) were shown in Fig. 2(c). Since the planes of these terraces correspond to the horizontal faces of the lamellae, therefore the height difference

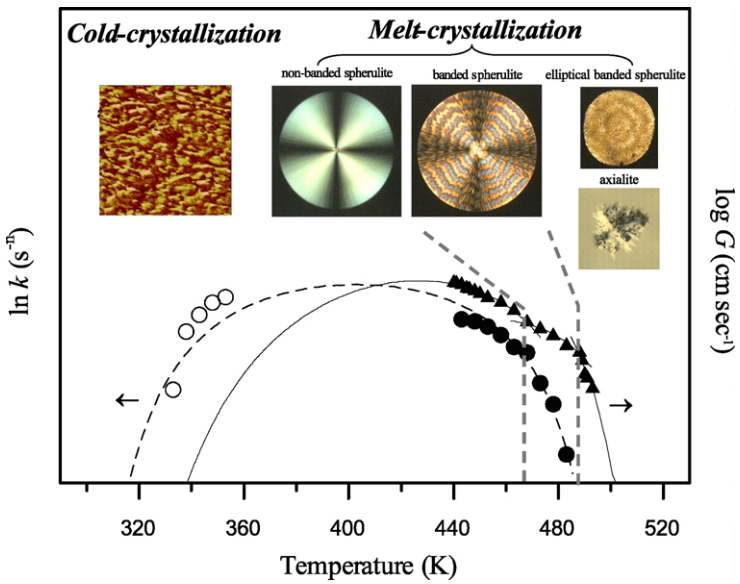

Fig. 1. Crystallization kinetics and the related morphologies of PTT thin film crystallized at various conditions: (●) Avrami rate constants from melt-crystallization; (○) Avrami rate constants from cold-crystallization; (▲) optical microscopy spherulitic growth rate. The morphology for cold-crystallized film was observed from a 250×250 nm^2 AFM phase image. The morphology for melt-crystallization was obtained by PLM.

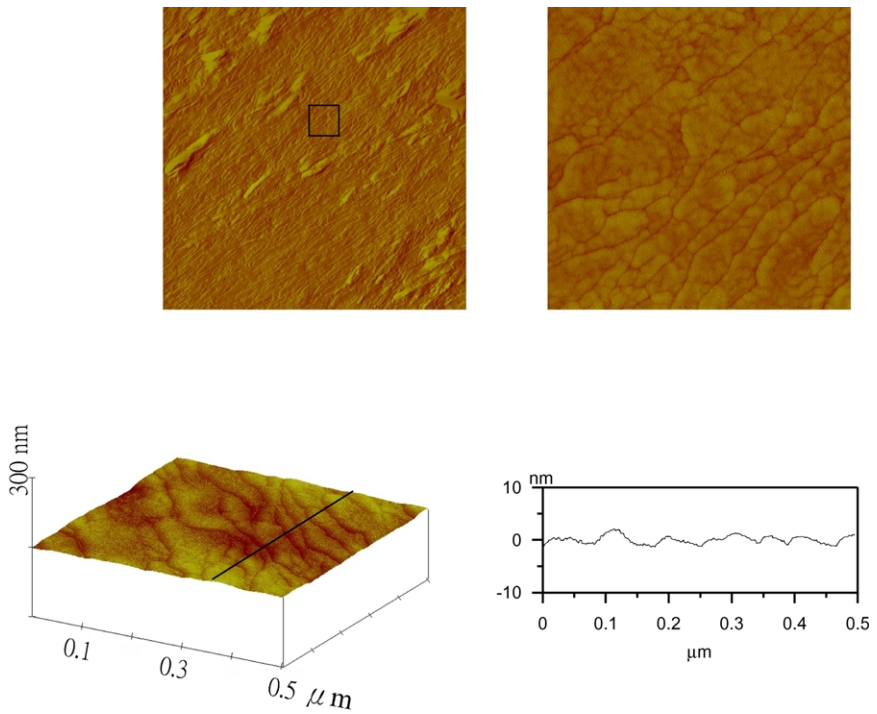

Fig. 2. AFM images obtained on the surface of a PTT non-banded spherulite crystallized at $T_{iso} = 453$ K: (a) phase image of 5×5 μm^2; (b) phase image of 500×500 nm^2 for the boxed region of (a); (c) three-dimensional image of (b); (d) the height profile along the black line in (c).

between the terraces also corresponds to the lamellar thickness. The flat-on lamellae were found to pile up into terrace-like layers with an average lamellar thickness of ca. 4 nm, obtained from the cross-sectional height profile of Fig. 2(d). In non-banded spherulites, the flat-on lamellae are slightly tilted and really not absolutely parallel to the substrate plane.

3.3. Banded spherulites

When PTT was crystallized at $T_{iso} = 468–488$ K, banded spherulites were formed. Fig. 3(a) showed the cross polarized optical micrograph of banded spherulites. The birefringence of spherulites with a Maltese cross and a distinct pattern of concentric rings are apparent. Fig. 3(b) shows the banded spherulite's texture when the sample's free surface was viewed by reflected light microscopy (RLM). The concentric rings can also be seen clearly. Ho et al. [52] suggested that the banded spherulite of PTT has a wave-like surface. The dark band and bright band in Fig. 3(b) correspond to the band of weak birefringence and the band of strong birefringence in Fig. 3(a), respectively. This can be easily convinced by arrow mark in Fig. 3(a) and (b). In Fig. 4(b), the three-dimension height image in AFM manifested that the PTT banded spherulite has a wavy-like morphology with alternating surface of 'ridges' and 'valleys' (see Fig. 4(a)'s boxed region). To compare with Fig. 4(a) and (b), it indicates that the surface of banded spherulite is considered to be consisted of alternate convex and concave bands. Besides, the dark and bright bands of

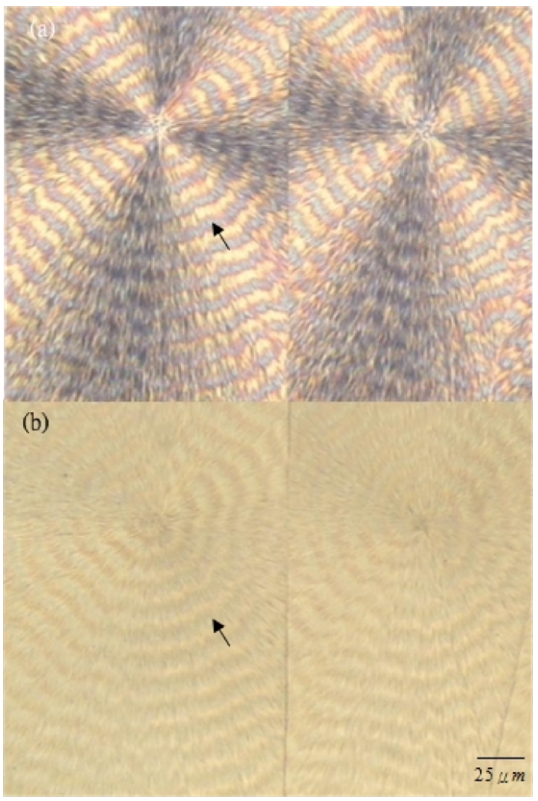

Fig. 3. Optical micrographs of PTT crystallized at 468 K (a) under polarized light microscope (b) under reflected light microscope.

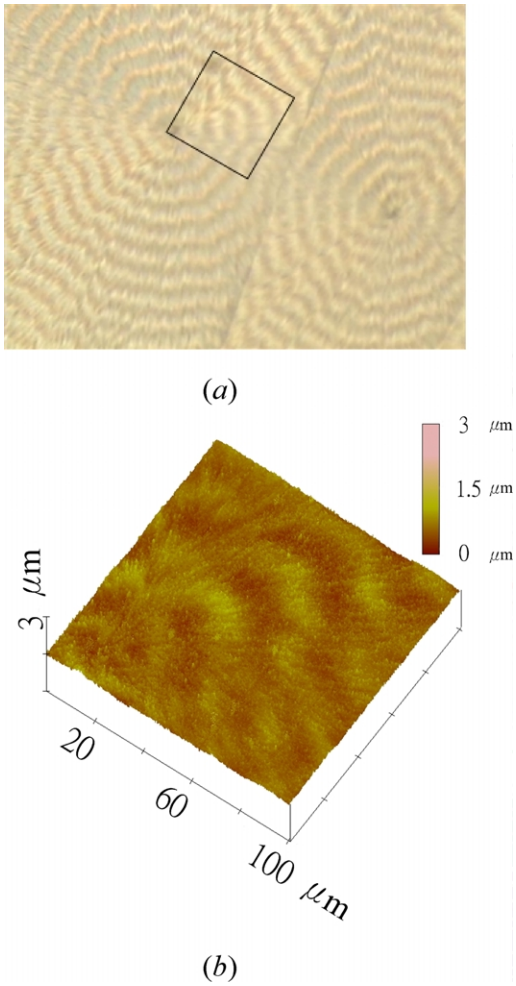

Fig. 4. (a) Reflected light micrograph of the free surface of PTT banded spherulite crystallized at $T_{iso} = 483$ K. (b) Three-dimensional AFM image of a quadrant of the banded spherulite corresponding to the boxed region in (a).

banded spherulite in RLM (Fig. 4(a)) correspond to convex and concave bands in AFM (Fig. 4(b)), respectively.

Fig. 5(a) and (b) are a series of AFM micrographs of the spherulite's concave band magnified from Fig. 4. Phase image of Fig. 5(a), 5×5 μm^2 scan size, shows that the surface of the concave band is rather smooth. Fig. 5(b) (scan size of 1×1 μm^2) gives a magnified view of the boxed region in Fig. 5(a). Fig. 5(c) is a three-dimensional height image from the boxed region of Fig. 5(b). It showed that the spherulite had regions of flat-on lamellae and multi-layered terrace-like morphology. The lamellar thickness, measured from the cross-sectional height profile between the horizontal planes of the terrace-like lamellae, was ca. 4 nm as shown in Fig. 5(d).

We now examined the convex bands of PTT banded spherulite. Fig. 6(a)–(d) showed a series of phase-resolution images of the convex band under various magnifications. Fig. 6(a), 14×14 μm^2 scan size, showed the organization of the fibrils that were oriented edge-on and parallel to the spherulite's growth direction. At a higher magnification of 5×5 μm^2 scan size, the boxed region of Fig. 6(a) showed an almost parallel fibrillar texture, Fig. 6(b). The average width of the fibril was about 500 nm. In order to investigate the lamellar organization within the fibrils, the microstructures were examined with a higher magnification at nanoscale level. Fig. 6(c), 500×500 nm^2 scan size, showed that the fibrils, which lied parallel with each other and formed the fibrillar stacks, were made up of edge-on lamellar bundles. Fig. 6(d), 125×125 nm^2 scan size, further showed the fibrils formed near the surface and a lamellar thickness of ca. 4.5 nm. The AFM observations showed that the convex band of banded spherulite was mainly consisted of fibrillation of edge-on lamellae.

3.4. Axialite crystallites and elliptical spherulites

In the early stage crystallization at a higher temperature of $T_{iso} = 490$ K, PTT formed axialite. AFM observation showed that the axialite was mainly made up of fibrils as shown in Fig. 7. Initially, the fibrils formed a framework similar to that found in a dendritic crystallization; the flat-on lamellae, indicated by the arrow in Fig. 7, then filled up the spaces of the intervening channels. When the sample was crystallized isothermally for ca. 20 h at 490 K, the axialite grew into an elliptical spherulite. Thus the axialite is a PTT crystallite at early stage crystallization.

Fig. 8 shows an optical micrograph of the elliptical spherulite under cross-polars. The elliptical spherulite had irregular, bushy concentric bands, but it did not exhibit the typical Maltese-cross extinction pattern. This morphology may be considered as an immature spherulite. In our observation, the banded characteristic of an elliptical spherulite is analogous with that of banded spherulites, i.e. the band of strong birefringence and band of weak birefringence correspond to concave band and convex band, respectively, in PTT elliptical spherulite. The lamellar organizations within these bands were also investigated using AFM observation.

Fig. 9(a) and (b) show the height and phase images of the elliptical spherulite concave band, respectively. The scan size of the image is 5×5 μm^2. However, at this magnification the lamellar organization could not be clearly observed. The boxed region of Fig. 9(a) was magnified to a scan size of 1.15×1.15 μm^2 to obtain a better resolution of the height image of Fig. 9(c). At this magnification the flat-on lamellae could now be discerned. The lamellae were found to grow along the radial direction and their arrangement was parallel to the substrate plane to form a terrace-like feature, though, the flat-on lamellae were not absolutely parallel to the substrate. Fig. 9(d) shows a cross-sectional height profile of these terraces. The average lamellar thickness obtained from the profile is ~5.5 nm. When the boxed region of Fig. 9(b)'s phase image was magnified to a scan size of 500×500 nm^2, Fig. 9(e), the soft, amorphous fold surface of the lamella was imaged as spotted regions. It can be seen that the lamellae in concave

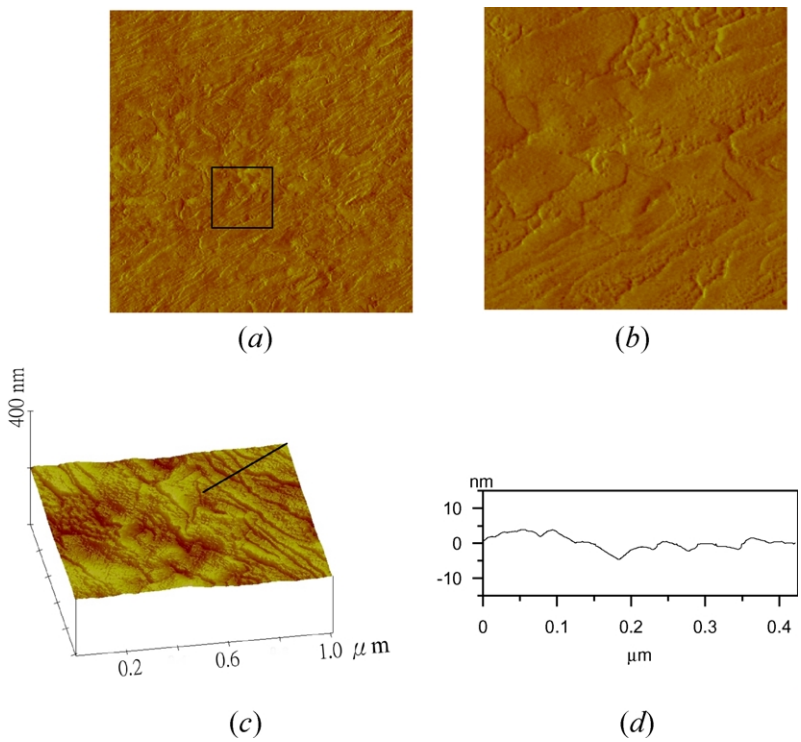

Fig. 5. AFM images obtained from the surface of the concave band of banded spherulite: (a) phase image of $5 \times 5\ \mu m^2$; (b) phase image of $1 \times 1\ \mu m^2$ for boxed region of (a); (c) three-dimensional image of (b); (d) the height profile along the black line in (c).

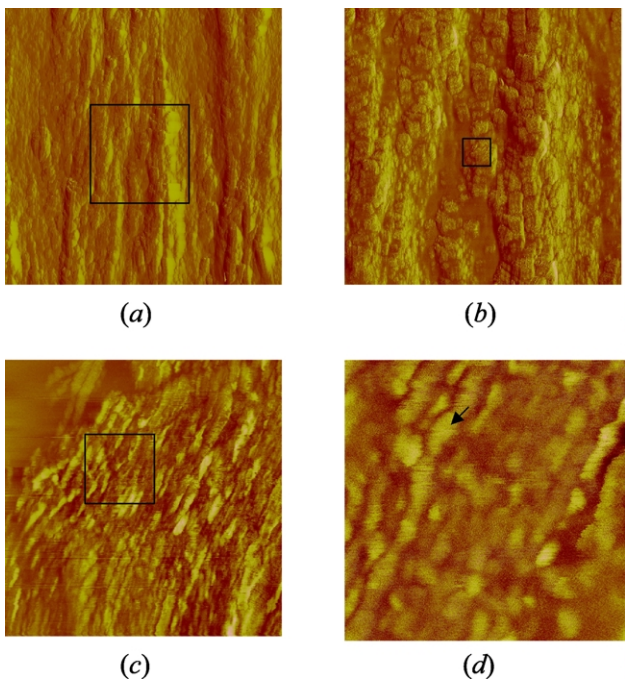

Fig. 6. A series of magnified images obtained on the surface of the convex band of banded spherulite: (a) phase image of $14 \times 14\ \mu m^2$; (b) phase image of $5 \times 5\ \mu m^2$ for the boxed-region of (a); (c) phase image of $500 \times 500\ nm^2$ for the box-region of (b); (d) phase image of $125 \times 125\ nm^2$ for the boxed-region of (c), the edge-on lamellae indicated by arrow mark.

band were also flat-on like those found in the concave band of banded spherulite in Fig. 5.

Fig. 10(a)–(c) are phase images of the elliptical spherulite's convex band at various magnifications. In Fig. 10(a), $14 \times 14\ \mu m^2$ scan size, the edge-on surface was very rough and the texture exhibited the appearance of the dendritic fibrils splayed apart from the dendritic branches in order to fill up the spaces along the radial direction. To resolve the structural feature of these fibrils, the boxed region of Fig. 10(a) was magnified in succession into Fig. 10(b)–(d) with $5 \times 5\ \mu m^2$, $1 \times 1\ \mu m^2$ and $125 \times 125\ nm^2$ scan sizes, respectively. Each image was magnified from the, respectively, boxed region of the previous figure. With a scan size of $125 \times 125\ nm^2$, Fig. 10(d) was able to show

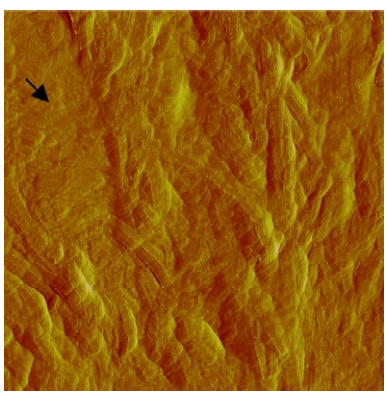

Fig. 7. AFM phase image ($14 \times 14\ \mu m^2$) obtained on the surface of the axialite; the arrow indicates the flat-on lamellae.

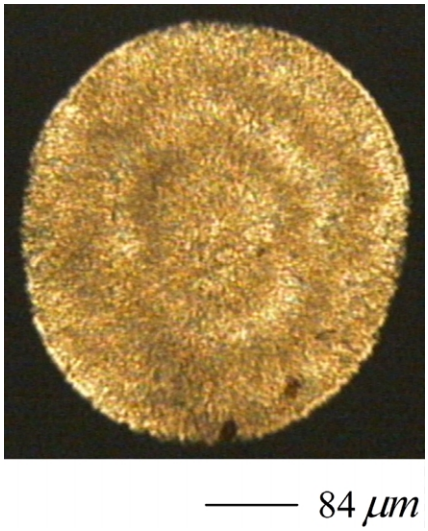

Fig. 8. PLM micrograph of an elliptical-shaped PTT spherulite crystallized at $T_{iso} = 490$ K for 20 h.

details of the fibril's lamellar morphology at nano-scale level. The arrow indicates the stiff (light) regions where the lamellae were edge-on i.e. lamella is perpendicular to substrate. The softer amorphous phase between the edge-on lamellae appeared on the shadowed regions. Fig. 10(d) also showed that the fibrillar bundles formed from the edge-on lamellae were arranged along the fibril's growth direction. The average thickness of these lamellae was ca. 5 nm. These features showed that the convex band in elliptical spherulite was made up of fibrils formed from the edge-on lamellae.

4. Discussion

4.1. Macro–micro morphological interplay

The macroscopic morphology is composed through microscopic structure of the lamellae. The question is how the microscopic organizations of the lamellae influence macroscopic patterns as crystallization temperature is varied. The AFM results showed that PTT's axialite, elliptical, banded and non-banded spherulites in the three regions of T_{iso} exhibit two basic types of lamellar organizations, i.e. the flat-on lamellae spread out to be terrace-like morphology and the edge-on lamellae aggregated to form fibrillar bundle. The terrace-like lamellae were found in the concave bands of banded spherulite (Figs. 5 and 9) and in non-banded spherulite (Fig. 2). On the other hand, the fibrillar bundles were found in the axialite and in the convex bands of banded spherulite (Figs. 6, 7 and 10). The lamellar thicknesses of the flat-on and the edge-on lamellae, measured from phase height AFM, were ca. 4–5 nm. These values were consistent with the SAXS results reported in our previous study [53].

In PTT spherulites the flat-on lamellae were constituted through multi-layering, followed by a non-coplanar growth on the exposed faces upon further crystallization. Such a growth pattern must have caused a giant screw dislocation and resulted in slip. When this occurs near the surface, a terrace-like feature is formed (Figs. 2, 5, and 9). The sliding of one lamella over another can be envisaged like the edges of the pages of a partly opened book. Current theories attributed dislocations to slips generated by stress-induced or thermal fluctuations [54,55]. Since chain folding occurs on the lamellar surfaces, the polymer chains must re-enter the crystal many times. The PTT terrace-like lamellae (Figs. 2(d), 5(d) and 9(d)) were not completely parallel to the substrate's surface but slightly tilted. The unequal surface stresses from chain tilting or staggered chain folding may give rise to a giant screw dislocation. As the lamellae piled up to form the terrace-like morphology, the giant screw dislocation generated a consistent sense in the terrace-like lamellae layers [17]. Thus giant screw dislocation is considered to be the most important defect in polymer crystallization, and is also a key feature of spherulitic proliferation in melt crystallization [14,20]. The flat-on lamellae were oriented along the radial direction. The intervening spaces were also filled up by these lamellae. Giant screw dislocation must also play a dominant role in the space filling of PTT spherulite via the propagation of the non-planar lamellae. The effectiveness of space filling depends on the frequency of the screw dislocations.

Fibrillar morphology was observed on PTT axialite and convex band of banded spherulites in thin films. These are structured by fibrils, which usually contain near hundred lamellae. The fibrils can be observed in the micrometer range, whereas lamellae usually have a dimension in the nanometer range. Fibrillation was formed by the aggregation of edge-on lamellae (Figs. 6, 7 and 10). Since the edge-on lamellae generate a larger specific surface area, fibrillation may be an essential process for relieving the surface free energy. Furthermore, fibrillar structure was not found in the non-banded spherulites, which consist of only the flat-on lamellae. These observations indicate that the fibrillar structure would be vanished at higher supercooling.

4.2. Origin of PTT banded spherulite formation

In PTT banded spherulites, two types of lamellar morphology were observed in the convex and concave bands surface, respectively. In the concave bands, the terrace-like lamellae were formed due to the giant screw dislocations. In the convex bands, the fibrils were formed from the edge-on lamellae. It can be seen that the edge-on and the flat-on lamellae are alternately generated to give rise to the periodic concentric rings observed in PLM and RLM. For a thin film crystallized with a free surface, the unrestrained lamellae generated periodic topographical variations [56,57] as they are developed along the radial direction of the banded spherulite. In Fig. 3(b), the wavy-like morphology of banded spherulite showed alternating surfaces of ridges and valleys. So far the study of wavy-like

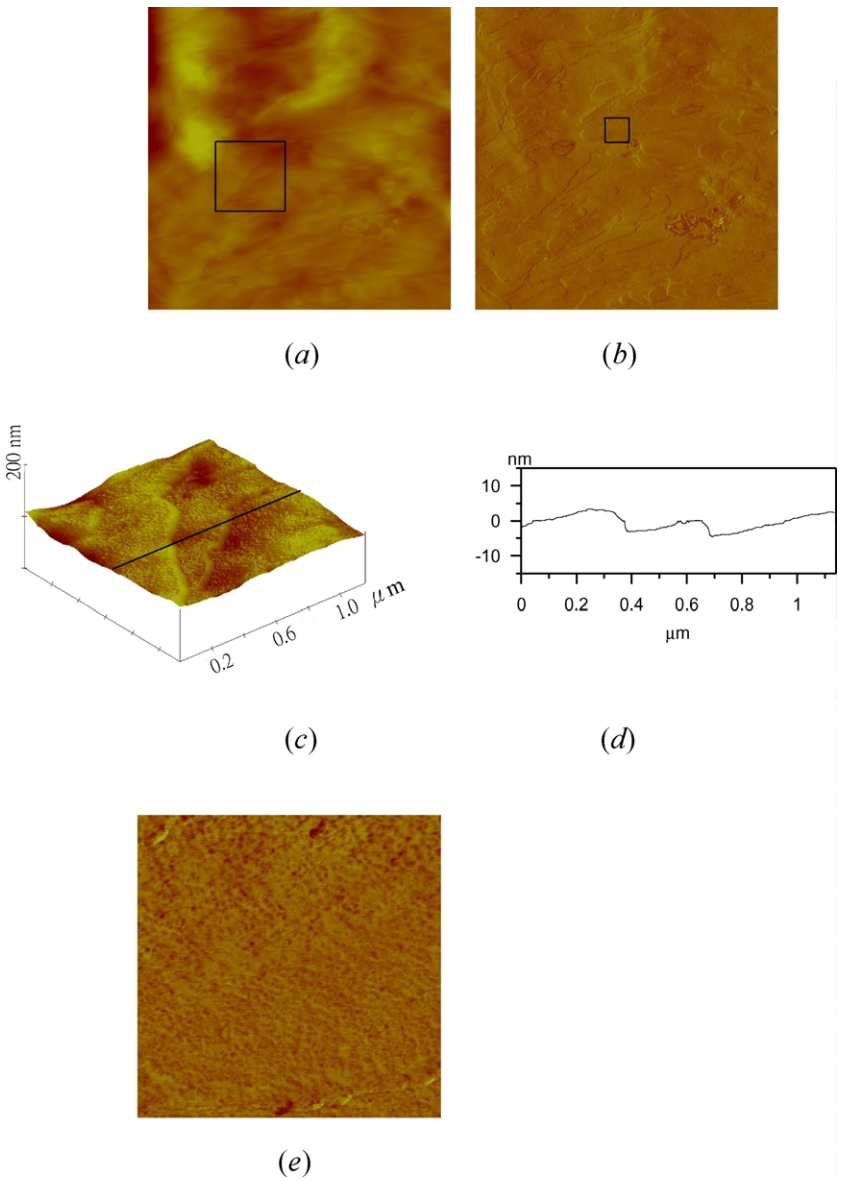

Fig. 9. AFM images obtained on the surface of the concave band of elliptically banded spherulite: (a) height image of $5 \times 5\ \mu m^2$; (b) phase image of $5 \times 5\ \mu m^2$; (c) three-dimensional image of an enlarged boxed region from (a); (d) height profile across the height image of (c); (e) phase image of $500 \times 500\ nm^2$ for the boxed region of (b).

surface on banded spherulites has been discussed superficially. Especially, there is an interesting problem how wavy-like surface forms as self-organization pattern. As discussed earlier we have confirmed that the convex band of PTT spherulite corresponds to PLM's dark band of weak birefringence and RLM's dark band. On the other hand, the concave band corresponds to PLM's bright band of strong birefringence and RLM's bright band. Therefore, the dark bands consist mainly of lamellae oriented preferably edge-on, whereas the most lamellae within bright bands are flat-on. There is a question why the generation of edge-on lamellae should exhibit the dark bands of weak birefringence /or extinction rings in PTT banded spherulite. Chuah [58,59] have studied on intrinsic birefringence of PTT in detail. It has been known that the growth or radius direction of PTT spherulite is *a* axis [52]. From the refractive indices along *a*, *b* and *c*-axis of PTT unit cell, the birefringence between parallel and perpendicular to radius direction of the spherulite could be zero as the edge-on lamellae need only to periodically tilt a little to get into extinction [59]. Since the fibrillation of edge-on lamellae were formed in the ridge region (dark bands in PLM) while the terrace-like lamellae were formed in the valley region (bright bands in PLM), we could suggest that the alternate organization of the edge-on and the flat-on lamellae in PTT banded spherulite is composed of two growth mechanisms. Recently, Wu and Woo [60] also reported that PTT banded spherulites are characterized with two alternating textures.

Fig. 11 shows the radius of PTT banded spherulite as a function of crystallization time at $T_c = 483$ K. The average

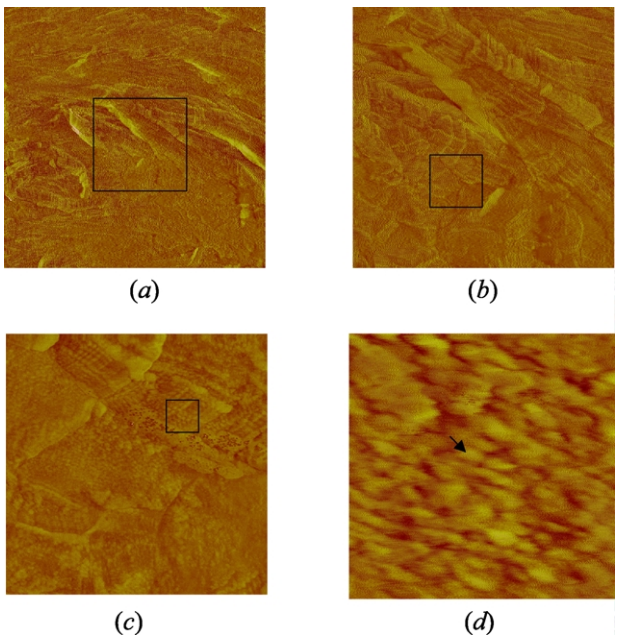

Fig. 10. A series of magnified images obtained on the surface of the convex band of elliptically banded spherulite: (a) phase image of 14×14 μm^2; (b) 5×5 μm^2 phase image for the boxed-region of (a); (c) 1×1 μm^2 phase image for boxed-region of (b); (d) 125×125 nm^2 phase image for the boxed-region of (c); the arrow indicates the twisted edge-on lamellae.

growth rate G is fitted from all experimental data with a slope of ~0.08 μm/sec. The true circles and vacated circles corresponded to the results of convex bands and concave bands, respectively. It is found that the slope of each convex band is smaller than that of the concave band, indicating that the growth rate was not constant. Two growth rates alternately appeared as PTT banded spherulite grew. This periodic change in growth rate is so-called rhythmic growth [30,61–63]. The various growth rates were specified that there is an obviously different growth mechanism between convex and concave bands. Directly perceived through the senses, slow growth of the convex bands could be reasonably attributed to the formation of ridge surface. Therefore, these experimental facts lead us to believe that the rhythmic growth of alternate concave and convex bands is essential to the growth process of PTT banded spherulites.

A number of studies had attempted to give an alternative explanation of the concentric extinction phenomena in

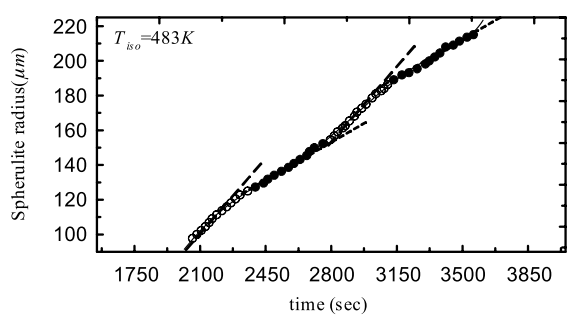

Fig. 11. Rhythmic growth for PTT banded spherulite at $T_{iso} = 483$ K (●) convex band (○) concave band.

terms, for example, of assumed preferred lamellar twisting [1,9] or of rhythmic crystallization [30,61–63]. It is important to note that the fibrillation of edge-on lamellae exhibit an abrupt change to be terrace-like flat-on lamellae along the radius of banded spherulite of PTT. Not only microscopic structure variation, moreover, the growth of PTT banded spherulites was also accompanied with rhythmic growth, which is characterized by a fast growth followed by a slow growth. One can then go on to appreciate that the deceleration of growth rate in convex band may be due to the growth habit of fibrillation of edge-on lamellae for forming a ridge surface. Meanwhile, the acceleration of growth rate in concave band may be attributed to the growth habit of terrace-like or flat-on lamellae for forming a valley surface. Consequently, our observation on rhythmic growth in PTT banded spherulites strongly supports the viewpoint of sharply alternating growth of edge-on to flat-on lamellae.

A large number of investigations have been performed concerning the banded spherulite, but many unsolved problems remain about the relationship between the morphology and growth mechanism. In the present study, however, the rhythmic growth signifies that the origin of PTT banded spherulite may be incompatible with the model of continuously lamellar twisting [1,9]. In fact, the formation of banded spherulite of PTT, which is really not advance formed lamellae and then twisting, changes lamellar habits at fixed distance or time. The growth of spherulite is completed by the need of cooperative movements of the large number of connected monomers. Therefore, the point we wish to emphasize is that the deposition of the stem and attachment of following stems in the folding chain on growth front may be a crucial role for forming a banded spherulite. That is, the process of stretching the stems in order to form edge-on or flat-on lamellae determines the lamellar growth mechanism. It may be nearer the truth to say alternating growth mechanism in PTT banded spherulites; i.e. alternating flat-on to edge-on mechanism.

The question that we must consider next is the cause of alternating change of lamellar growth habits in PTT banded spherulites. We conjecture that there may communicate some message to the crystal/melt interface during the formation process of PTT banded spherulite. Accordingly, the effects of self-generated field on polymer crystallization [64] perhaps provide a consideration to the formation mechanism of PTT banded spherulites. The act of crystallization normally creates fields in *stress*, *composition*, and *thermal* fields can feed back strongly to affect the kinetics and morphology of the crystallizing material [64]. The continuous lamella with helicoidal twisting [1,9] that has an effect of stress field. On the other hand, Okabe et al. [65] reported that the referential rejection of PVAc chains into the inter-spiral (inter-ring) regions of the growing ringed spherulite during PVDF crystallization in polymer blends

that may be considered related to the effect of compositional fields.

However, not only the effect of stress and composition field but also that of thermal field could provide an opportunity to form banded texture. It should be mentioned here that the occurrence of 'banded texture' is a rather common phenomenon to many rapid solidification alloys [28,29]. The banded textures are usually characterized by alternate bright and dark bands parallel to the solidification front [28]. The bight band is formed from microsegregation-free structure; in contrast, the dark band is formed either cellular or dendritic structure. The fast and slow growth rates are, respectively, found in the bright and dark bands. In principle, the crystallization from the melting growth is accompanied by release of latent heat, since the crystalline state has lower entropy. The physical origin of this effect can be understood qualitatively by noting that the liberation of the latent heat at the crystallization front allows the front to advance rapidly, but the material behind the front cannot keep up and then crystal growth slows down until more heat can diffuse to the boundary. This indicates that diffusion process of latent heat at the crystal/melt interface may play a role for the formation of banded texture. The effect of latent heat diffusion is a truth little understood in the morphology of the polymer but it is a very essential subject. In fact, the physical origin of the banded texture has not been elucidated with certainty. It probably shares some common principle with other systems. The effect of latent heat diffusion giving an idea of that formative mechanism of banded spherulites in PTT maybe analogized with banded morphology in solidified alloys. They have a consistent phenomenon characterized by periodic variation of growth mechanism along growth direction. Although a similar growth mechanism in banded morphology of alloys does not automatically guarantee whether the origin is the same. It is worthily investigating the banded forming aspects of polymeric crystallization from a new perspective. The latent heat diffusion may be a candidate to explain the cause of PTT banded spherulites.

4.3. Self-organization of PTT banded spherulite

A model, schematically illustrated in Fig. 12, can now be constructed to summarize the hierarchic structure of PTT banded spherulites at different length scales. In the intrinsic sense of polymer crystallization that the crystallites formed at a given temperature do usually not obtain their equilibrium properties owing to temperature dependence of lamellae thickness. The crystalline state of polymer matter in most cases indicates a metastable structure produced by a non-equilibrium growth process. PTT banded spherulites can even be regarded as a self-organization process since a hierarchy of patterns on various length scales are formed ranging from crystalline stems on the nanometer scale up to spherulite size of hundreds microns. At the molecular level, the chains form a regular lattice with fixed spacings between the lattice sites. At this microscopic level scale, the ordering of the molecular chains from X-ray or electron diffractions showed the atoms and molecular chains of PTT are arranged in a triclinic crystal lattice [66]. At a nanometer length scale, AFM revealed two types of lamellar growth. The flat-on lamellae, caused by giant screw dislocations, formed the terrace-like lamellae within the valleys of the concave bands. The fibrillar texture, consisted of edge-on lamellae, was found in the ridges of the convex band. The above microstructures were formed from two distinct growth mechanisms coexisting within the banded spherulite.

As the morphological formation of PTT banded spherulites is discussed above, the wavy-like surface, alternating growth habit and rhythmic growth are found as the spherulite grows. To note that the banded spherulite is formed through the microscopic coordination of the lamellar crystal to macroscopic ordering, and the banded texture suddenly disappeared below $T_{iso} = 468$ K. A question that has been touched on but not explored is how the cooperation of these lamellae brought about the spatial or temporal patterns at a macroscopic level for the banded spherulite. This phenomenon may be considered in the light

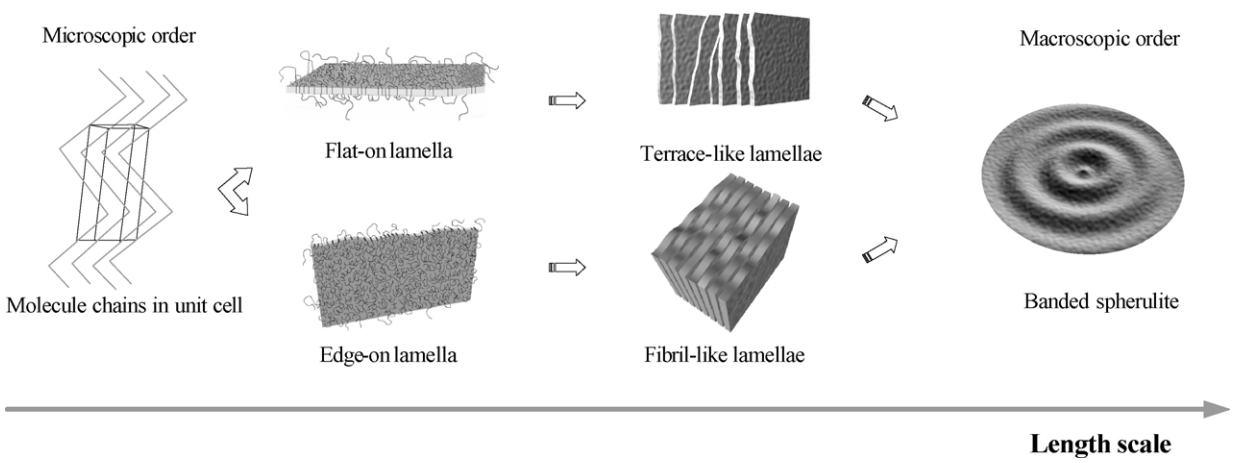

Fig. 12. Schematic model of hierarchic structure in the formation of PTT banded spherulite.

of the formation of complex space-time self-organization patterns in a non-equilibrium process [22,23]. The terms 'Dissipative structures' [22] and 'Synergetics' [23] have been widely accepted to indicate the crucial role of simultaneously cooperative process as a necessary prerequisite for a system to undergo a sudden change of properties and symmetry at critical thermodynamic values arising in far-from-equilibrium conditions. Following this viewpoint, regardless of lamellar twisting model or alternating growth model, the banded spherulites perhaps exhibit a common characteristic of synergetics that may be a candidature for dissipative structures. Recently, a viewpoint of crystallization under non-equilibrium conditions has been extensively accepted in polymer crystallization [48,67]. According to the reasoning from analogy among those systems as mentioned above, we thus proposed that PTT banded spherulites formed from thin film crystallization exhibit a microscopic cooperation of lamellar organization, which transforms into a macroscopic order of periodic banded structure as the self-organization under non-equilibrium crystallization.

4.4. BNB morphological transition as a non-equilibrium phase transition

Fig. 13 shows a PLM observation of PTT spherulite crystallized in steps of distinct T_{iso}. The sample was isothermally crystallized in sequence at 489, 468 and 453 K. The center of the spherulite clearly showed an axialite-like structure ($T_{iso} = 489$ K). A banded texture was formed when the temperature was lowered to $T_{iso} = 468$ K. Finally, a non-banded texture was formed as the temperature was further lowered to 453 K. When T_{iso} is varied, the morphology is sharply changed to another one at once. This result demonstrates that there might be a threshold of supercooling temperature at which a morphological transition would take place.

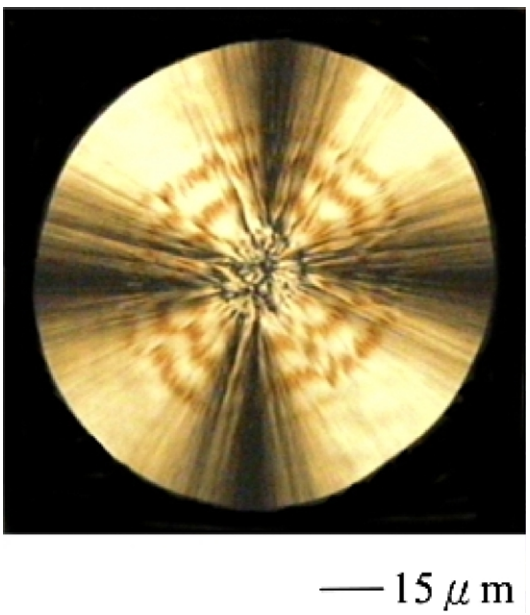

Fig. 13. PLM micrograph of PTT spherulite successively crystallized under a series of T_{iso} (489 K → 468 K → 453 K).

For the present, we shall confine our attention to BNB morphological transition. Recently, Hutter and Bechhoefer [46,47] have suggested that the transition from non-banded spherulite to banded spherulite in liquid crystal exhibits a characteristic analogous to the second-order morphological transition and shows a critical behavior. However, Ben-Jacob et al. [39] term the transitions where the growth rate discontinuously jumps as the first-order morphological transition and those where the slope of growth rate discontinuity as the second-order morphological transitions. In many systems, researchers have introduced the idea of morphology/phase transitions [38–41,68–72]. These concepts, borrowed from the theory of equilibrium phase transition, suggest that various non-equilibrium structures emerge upon varying the parameters (such as undercooling, anisotropy etc.) governing the growth process. In the present work, we presuppose that BNB morphological transition may vary non-analytically with ΔT, in analogy with non-equilibrium phase transition, having a critical phenomenon. The periodic spacing of band suddenly dissipated at $\Delta T = 58$ K where BNB morphological transition appears. This divergence is analogous with a critical phenomenon, which one may expect to exhibit the second-order transition. It further implies the existence of morphological transitions; that is, a sharp transition between morphologies occurs with a varying of the growth conditions. If this presupposition could be accepted, one can assume that periodic spacing of band may be referred to be an order parameter. The order parameter plays a center role for critical point in non-equilibrium phase transition. Generally, in non-equilibrium phase transition the change of one phase to another was taken place suddenly at one point, indicating a saltation process. Non-equilibrium phase transition has a common characteristic of order parameter, which continuously changes to zero or vanishes to non-zero at critical point.

Let us look at BNB morphological transition in PTT from a new perspective of non-equilibrium phase transition. If we assume that, the banding formation has a feature of critical behavior. For the interpretation on our result, the appropriate expression for the relative distance to the threshold is $\varepsilon = (T - T_c)/T_c$, where the T_c is the critical temperature of BNB morphological transition. In this work, we define the temperature of 467 K at which banded spherulite disappears at T_c. Banded spherulite emerges a macroscopic ordering, and the transition corresponds to the broken symmetry. BNB morphological transition could be regarded as a macroscopic order-to-disorder transition. The macroscopic order phase cannot exist below T_c, either as metastable or unstable state. This is a characteristic feature of non-equilibrium phase transition. The periodic spacing is a function of temperature and then it vanishes as temperature

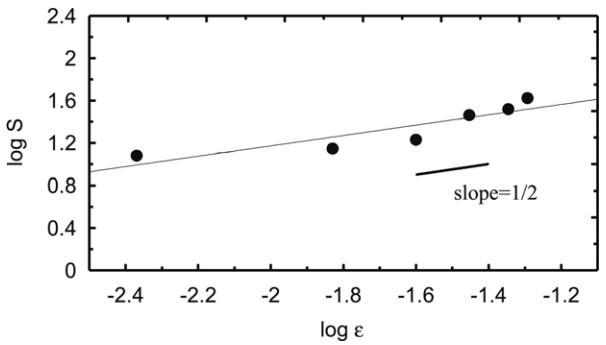

Fig. 14. Logarithmic plot of the space period S versus $\varepsilon = (T - T_c)/T_c$.

approaches to T_c :

$$S \sim \begin{cases} 0 & \text{for } T < T_c \\ \varepsilon^{\bar{\beta}} & \text{for } T > T_c \end{cases} \quad (1)$$

The periodic spacing S is characterized by a new exponent $\bar{\beta}$.In Fig. 14, the periodic spacing is plotted as a function of the relative distance to the threshold. As that expected with respect to Eq. (1), a power law behavior is found. Within experimental error, the slope of the straight line is close to 1/2. This value could be compared with the well-known critical exponent $\beta = 1/2$ for the order parameter in the mean-field theory. Therefore, expanding the periodic spacing as a power law in the reduced temperature, critical exponent can be defined by analogy with the mean-field theory of equilibrium phase transition [44,45]. Concerning this viewpoint, there is a rather common belief in the literatures [73–79] that non-equilibrium phase transitions bear basically a classical character, i.e., they can be described, even exactly for experimental data, on the basis of the classical Landau theory of phase transition and critical phenomena. To our knowledge, the critical exponent in BNB morphological transition has not hitherto been defined. It may explain the surprising fact that quite different systems are governed by the same theorem for the order parameters. Although, theories of broken symmetry and renormalization groups demonstrate that emergent macro-phenomena are not merely the logical consequence of microphysical laws. The microstructures may affect the ways of various systems close to their respective critical temperature, which may be described by a universal critical exponent and simple scaling law. All of these identify BNB morphological transition as a kind of non-equilibrium phase transition. Although, non-equilibrium and equilibrium phase transitions are based on different background of theory. They have been pointed out that enhancement of fluctuations, long-range order and critical slowing down are common to both equilibrium and non-equilibrium critical phenomena. These common characteristics by no means fortuitous among them must have interplay between macro- and micro-structure.

5. Conclusion

In spite of various origins for the formation of banded spherulite, there have three universal phenomena under isothermal crystallization: (1) the morphological change from banded to non-banded depends on the supercooling, and there might be a threshold value for the supercooling. (2) Although, the dependence of BNB morphological transition on supercooling varies significantly with material under consideration, the periodic spacing generally increases with decreasing ΔT in the banding region, i.e. the slow growth rate would lead to larger periodic spacing. (3) The periodic spacing of banded spherulite, which is constant for isothermal crystallization, has no dependence on the spherulite size. Underlying the universality as mentioned above, we believe that there may be a set of overarching principles lending a unified perspective for banded spherulites. Nevertheless, the BNB morphological transition in spherulite formation has been regarded as a kind of non-equilibrium phase transitions in the present work; we still have a long way to go before we verify a clear definition in the universality of banded spherulite.

References

[1] (a) Keller A. J Polym Sci 1955;291:17. (b) Keller A. J Polym Sci 1959;39:151.
[2] (a) Keith HD, Padden Jr. FJ. J Polym Sci 1959;39:101. (b) Keith HD, Padden Jr. FJ. J Polym Sci 1959;39:123.
[3] Price FP. J Polym Sci 1959;39:139.
[4] Bassett DC. Principles of polymer morphology. Cambridge: Cambridge University Press; 1981.
[5] Lindenmeyer PH, Holland VE. J Appl Phys 1964;35:55.
[6] Ryschenkow G, Faivre G. J Cryst Growth 1988;87:221.
[7] Bisault J, Rysschenkow G. J Cryst Growth 1991;110:889.
[8] Bechhoefer J, Hutter JL. Physica A 1998;249:82.
[9] Barham PJ, Keller A. J Mater Sci 1977;12:2141.
[10] Bassett DC, Hodge MA. Proc R Soc Lond 1981;A377:25.
[11] Patel D, Bassett DC. Polymer 2002;43:3795.
[12] Hoffman JD, Lauritzen JI. J Res Natl Bur Stand 1961;65A:297.
[13] Keith HD, Padden Jr. FJ. Polymer 1984;25:28.
[14] Toda A, Keller A. Collid Polym Sci 1993;271:328.
[15] Toda A, Arita T, Hikosaka M. Polymer 2001;42:2223.
[16] Bassett DC, Vaughan AS. Polymer 1985;26:717.
[17] Bassett DC, Olley RH, Al Raheil IAM. Polymer 1988;29:1539.
[18] Organ SJ, Keller A. J Mater Sci 1985;20:1571.
[19] Keith HD, Padden Jr. FJ. Macromolecules 1996;29:7776.
[20] Keith HD. Polymer 2001;42:9987.
[21] Cross MC, Hohenberg PC. Rev Mod Phys 1993;65:851.
[22] Glansdorff P, Prigogine I. Self-organization in non-equilibrium systems. New York: Wiley; 1977.
[23] Haken H. Synergeics. Berlin: Springer; 1978.
[24] Lefaucheux F, Robert MC, Bernard Y. J Cryst Growth 1988;88:97.
[25] Boettinger WJ, Shechtman D, Schaefer RJ, Biancaniello FC. Metall Trans A 1984;15:55.
[26] Coriell SR, Sekerka RF. J Cryst Growth 1983;61:499.
[27] Merchant GJ, Davies SH. Acta Metal Mater 1990;38:2683.
[28] Carrard M, Gremaud M, Zimmermann M, Kurz W. Acta Metall 1992;40:983.

[29] (a) Karma A, Sarkissian A. Phys Rev Lett 1992;68:2616. (b) Karma A, Sarkissian A. Phys Rev E 1993;47:513.
[30] Kyu T, Chiu HW, Guenthner AJ, Okabe Y, Saito H, Inoue T. Phys Rev Lett 1999;83:2749.
[31] Ben-Jacob E, Levine H. Nature 2001;409:985.
[32] Hong PD, Chuang WT, Hsu CF. Polymer 2002;43:3335.
[33] Keith HD, Padden FJ. J Polym Sci Part B 1987;25:2371.
[34] Scandola M, Ceccorulli G, Piaaoli M, Gazzano M. Macromolecules 1992;25:1405.
[35] Delaite E, Point JJ, Damman P, Dosière M. Macromolecules 1992;25:4768.
[36] Singfield KL, Brown GR. Macromolecules 1995;28:1290.
[37] Hoffman JD. Polymer 1983;24:3.
[38] Ben-Jacob E, Garik P, Mueller T, Grier D. Phys Rev A 1988;38:1370.
[39] Ben-Jacob E, Garik P. Nature 1990;343:523.
[40] Shochet O, Ben-Jacob E. Phys Rev E 1993;48:R4168.
[41] Saito Y, Müller-Krumbhaar H. Phys Rev Lett 1995;74:4325.
[42] Nitzan A, Ortoleva P. Phys Rev A 1980;21:1735.
[43] Nicolis G, Malek-Mansour N. Prog Theor Phys Suppl 1978;64:1.
[44] Sornette D. Critical phenomena in natural sciences. New York: Springer; 2000.
[45] Auyang SY. Foundations of complex system theories. New York: Cambridge University Press; 1998.
[46] Hutter JL, Bechhoefer J. Phys Rev Lett 1997;79:4022.
[47] Hutter JL, Bechhoefer J. Phys Rev E 1999;59:4342.
[48] Magonov SN, Whangbo MH. Surface analysis with STM and AFM. Weinheim: VCH; 1996.
[49] Hong PD, Chung WT, Hsu CF. Polymer 2002;43:3335.
[50] Fu Q, Heck B, Strobl G, Thomann Y. Macromolecules 2001;34:2502.
[51] Acierno S, Grizzuti N, Winter HH. Macromolecules 2002;35:5043.
[52] Ho RM, Ke KZ, Chen M. Macromolecules 2000;33:7529.
[53] Hong PD, Chung WT, Yeh WJ, Lin TL. Polymer 2002;43:6879.
[54] Frank FC, Read WT. Phys Rev 1950;79:722.
[55] Peterson JM. J Appl Phys 1966;37:4047.
[56] Singfield KL, Klass JM, Brown GR. Macromolecules 1995;28:8006.
[57] Markey L, Janimak JJ, Stevens GC. Polymer 2001;42:6221.
[58] Chuah HH. J Polym Sci Part B 2002;40:1513.
[59] Chuah, HH, Shell Chemical Company, USA, June; 2003, Private communication.
[60] Wu PL, Woo EM. J Polym Sci Part B 2003;41:80.
[61] Wang Z, An L, Jiang B, Wangh X. Macromol Rapid Commun 1998;19:131.
[62] Pawlak A, Galeski A. J Polym Sci Part B 1990;28:1813.
[63] Wang Z, An L, Jiang W, Jiang B, Wang X. J Polym Sci Part: B 1999;37:2682.
[64] Schultz JM. Polymer crystallization. New York: Oxford University Press; 2001.
[65] Okabe Y, Kyu T, Saito H, Inoue T. Macromolecules 1998;31:5823.
[66] Suzie PD, Perez S, Revol JF, Brisse F. Polymer 1979;20:419.
[67] (a) Ferreiro V, Douglas JF, Warren J, Karim A. Phys Rev E 2002;65:042802. (b) Ferreiro V, Douglas JF, Warren J, Karim A. Phys Rev E 2002;65:051606.
[68] Tu Y, Levine H, Ridgway D. Phys Rev Lett 1994;71:3838.
[69] (a) Brener E, Müller-Krumbhaar H, Temkin D. Phys Rev E 1996;54:2714. (b) Brener E, Müller-Krumbhaar H, Temkin D. Europhys Lett 1992;17:535.
[70] Ben-Jacob E, Godbey R, Goldenfeld ND, Koplik J, Levine H, Mueller T, Sander LM. Phys Rev Lett 1985;55:1315.
[71] Saeada Y, Dougherty A, Gollub JP. Phys Rev Lett 1986;56:1260.
[72] Ben-Jacob E, Garik P. Physica D 1989;38:16.
[73] Haken H. Advanced synergetics. Berlin: Springer; 1983.
[74] Graham R. In: Nicolis G, Dewel G, Turner JW, editors. Order and fluctuations in equilibrium and nonequilibrium statistical mechanics. New York: Wiley; 1981.
[75] Beijeren van H, Schulman LS. Phys Rev Lett 1984;53:806.
[76] Masi de A, Ferrari PA, Lebowitz JL. Phys Rev Lett 1985;55:1947.
[77] Krug J, Lebowitz JL, Spohn H, Zhang MQ. J Stat Phys 1986;44:535.
[78] Beysens D, Gbadamassi M. Phys Rev A 1980;22:2250.
[79] Leung K, Cardy JL. J Stat Phys 1986;44:567.